



Integrated molecular analysis of the inactivation of a non-enveloped virus, feline calicivirus, by UV-C radiation

Tsuyoshi Tanaka,* Osamu Nogariya, Nozomi Shionoiri, Yoshiaki Maeda, and Atsushi Arakaki

Division of Biotechnology and Life Science, Institute of Engineering, Tokyo University of Agriculture and Technology, 2-24-16 Naka-cho, Koganei, Tokyo 184-8588, Japan

Received 2 August 2017; accepted 25 January 2018
Available online xxx

UV-C treatment has been shown to be a powerful way to inactivate non-enveloped viruses in water samples. However, little is known about how the viruses were inactivated by UV-C radiation. In this study, we investigated the inactivation mechanism of a single-stranded RNA (ssRNA) non-enveloped virus, feline calicivirus (FCV), as a surrogate for the human norovirus, using UV-C radiation with different wavelengths. Integrated molecular analyses using RT-qPCR, sodium dodecyl sulfate-polyacrylamide gel electrophoresis (SDS-PAGE), and mass spectrometry were employed to evaluate the extent of ssRNA genome and protein degradation. UV-C radiation of FCV efficiently impaired the infectivity of FCV in mammalian cells. We also identified degradation of the RNA genome, whose copy numbers decreased from 48 to 56% following UV₂₅₅ or UV₂₈₁ radiation. Significant degradation of capsid protein was not observed, whereas oxidation of amino acid residues in the major capsid protein VP-1 was determined. Our results suggest that damage to the RNA genome is primarily responsible for the observed decrease in FCV infectivity of CRFK cells. This study provides not only relevant baseline data but also an overview and possible mechanism for the disinfection of non-enveloped ssRNA viruses using UV-C radiation.

© 2018, The Society for Biotechnology, Japan. All rights reserved.

[Key words: UV-C radiation; Feline calicivirus; Non-enveloped virus; RNA genome; Capsid protein]

Many intestinal infections are caused by waterborne or food-borne non-enveloped viruses, such as adenovirus, rotavirus, norovirus, and sapovirus (1). Disinfection of water and food supplies from these viruses is therefore an important issue to prevent gastroenteritis outbreaks (2,3). Non-enveloped viruses are surrounded by a stable protein coating and are resistant to heat, dryness, and chemical inactivants; in contrast, enveloped viruses are surrounded by both proteins and lipids and are less stable in harsh environmental conditions and treatments (4). Numerous methods for inactivation of non-enveloped viruses have been proposed and investigated, including heat, chemical, pH, and light treatments (5,6). UV-C radiation is a convenient and cost-effective inactivation method and appears to be effective for a wide variety of virus species (5). Although UV-C inactivates viruses by altering their genome or capsid proteins, most inactivation studies have focused their attention on the effect of wavelength and fluence on inactivation efficiency. A detailed mechanism for inactivation of viruses by UV-C radiation remains unclear.

Several previous studies have advanced the understanding of UV-C radiation-based inactivation of non-enveloped viruses. UV-C-induced single-stranded RNA (ssRNA) genome degradation was identified in a comparative inactivation study of poliovirus and other RNA phages (7). The observed genome degradation is proposed to be a main phenomenon of viral inactivation by UV-C radiation. Site-specific backbone cleavage of capsid proteins by

UV-C radiation was reported in a study of the ssRNA-genome virus bacteriophage MS2 (6). Damage to capsid proteins was found to inhibit injection of the viral genome into the host cell. UV-C radiation of the human adenovirus caused significant damage to its double-stranded DNA (dsDNA) genome but insignificant damage to virus proteins (8). More recently, the wavelength dependence of UV-C on ssRNA genome degradation of MS2 was investigated. Based on these results, damage in genomic RNA and proteins, RNA-protein crosslinking, or the occurrence single-strand RNA breaks was proposed (9). Thus, UV-C-induced inactivation of non-enveloped viruses is likely to be dependent on the virus type; however, the results are often contradictory or equivocal. Further systematic molecular analysis with various non-enveloped viruses is thus needed to understand the fundamental mechanisms governing the inactivation of viruses by UV-C radiation.

Here, we investigated the inactivation of a non-enveloped ssRNA virus, feline calicivirus (FCV), as a surrogate for the human norovirus. We showed that the use of copper iodide (CuI) nanoparticles can efficiently inactivate the infectability of FCV in animal cells (10). The high antiviral activity of CuI nanoparticles was shown to be attributable to Cu⁺, followed by reactive oxygen species generation and subsequent capsid protein oxidation. Moreover, we demonstrated the inactivation of FCV by electrochemical treatment in a newly-developed flow-cell equipped with a screen-printed electrode (11). The electrochemical treatment effectively inactivated FCV via oxidation of peptides in the structural region, causing structural deformation of virus particles. A common inactivation mechanism based on protein oxidation was found in the studies of two different inactivation methods. FCV was also shown to be

* Corresponding author. Tel.: +81 423 88 7021; fax: +81 423 85 7713.
E-mail address: tsuyo@cc.tuat.ac.jp (T. Tanaka).

sensitive to UV-C radiation (12), and its inactivation may involve RNA genome degradation and/or protein oxidation, although the mechanism has not yet been investigated.

In this study, we aimed to determine the effects of UV-C radiation on FCV inactivation by integrated molecular analyses using RT-qPCR, SDS-PAGE, and mass spectrometry. We used an light emitting diode (LED) capable of emitting different wavelengths as a source of UV-C radiation for FCV inactivation and analyzed the resulting changes in FCV capsid morphology and damages to the RNA genome and capsid proteins. Using the results from these multiple analyses, the inactivation mechanism of non-enveloped virus is discussed.

MATERIALS AND METHODS

Virus propagation FCV strain F-9 (ATCC VR-782) was propagated in Crandell-Rees feline kidney (CRFK) cells (ATCC CCL-94) in 6-well microtiter plates as previously described (11). Briefly, the cells were grown in Eagle's minimum essential medium (MEM) supplemented with 10% fetal bovine serum in 6-well titer plates. Confluent monolayers of the cells were inoculated with FCV, and then, 0.7% MEM agar was added to the wells, followed by 48 h of incubation at 34°C and 5% CO₂. The value of plaque-forming units per milliliter (pfu/mL) was determined from the average plaque numbers from 3 wells.

UV-C radiation of FCV FCV (approximately 1×10^8 pfu/mL) was suspended in phosphate buffered saline composed of 4.0 mM phosphate and 155 mM sodium chloride (pH 7.4), and 180- μ L aliquots were dispensed in a 96-well microtiter plate. The microtiter plate was then placed on a magnetic stirrer to homogeneously disperse FCV in the solution (Fig. 1). UV-C-LED (Sensor Electronic Technology, SC, USA) was placed on top of the microtiter plate and was electrically connected to a power supply (PMC250–0.25 A, Kikusui Electronic Corp., Yokohama, Kanagawa, Japan). UV-C-LEDs with peak wavelengths of UV₂₅₅ (245–271 nm), UV₂₆₁ (252–277 nm), UV₂₇₇ (266–292 nm), and UV₂₈₁ (270–297 nm) were used (Fig. S1). The distance between the UV-C-LED and the surface or bottom of the virus suspension was 5 and 11 mm, respectively. The emitting output power and wavelength were measured using an integrating sphere (SMS-500, Sphere Optics, Uhldingen, Germany). After

UV-C radiation, FCV suspensions were recovered to evaluate the effect of UV-C on plaque formation. Each sample was analyzed in 3 independent experiments using 3 plates.

The fluence (mJ/cm²) was calculated by multiplying the average irradiance of the sample (mW/cm²) by the exposure time. The average irradiance was calculated based on a correction factor, and the average irradiance was determined as described by Bolton and Linden (13). The reflection and water factors were used as the correction factors for the average irradiance. In this calculation, the petri factor was ignored since the radiation area was too small. The divergence factor was also ignored because the ratio of the distance between the surface of the virus suspension and the light source to the diameter of the well was significantly less than 4. A reflection factor for water (0.975) was used in accordance with a report by Bolton and Linden (13). The water factor accounted for the UV-C absorbance of the water through the sample water depth at 255, 261, 277, and 281 nm. The irradiance at the sample surface was the product of the reduction rate corresponding to the distance determined by the UV-C detector; the irradiance rate at the top of the well was calculated by the output power as measured by the integrated sphere technique.

Before using UV-C-LED in the experiments, the output powers of the UV-C-LEDs were determined. Because radiated light energies are dependent on the radiated wavelengths, radiation times for each UV-C wavelength (UV₂₅₅, UV₂₆₁, UV₂₇₇, and UV₂₈₁) were calculated based on the average irradiance rates. The conditions for different UV-C wavelengths with a magnitude of 40 mJ/cm² are listed in Table 1.

Transmission electron microscopy analysis FCV particles obtained from UV₂₅₅- or UV₂₈₁-radiated FCV suspensions were observed by transmission electron microscopy (TEM) (H7600; Hitachi, Japan). After subjecting samples to more than 100 mJ/cm² of radiation, an aliquot of FCV was stained with 2% uranyl acetate, followed by TEM analysis, operated at an accelerating voltage of 100 kV.

Quantitative PCR analysis Extraction of FCV RNA from non-treated and UV-C (UV₂₅₅ or UV₂₈₁) radiated samples was carried out using a QIAamp Viral RNA Mini Kit. Quantitative PCR (qPCR) was carried out using a real-time PCR system (Applied Biosystems). The FCV reverse primer 5'-CATATGCGCTCTGATGGCTTGAACTG-3' and forward primer 5'-TAATTCGGTGTGTTGATTGGCTGGGCT-3' amplify an 83 bp product from the ORF1 region of the FCV genome (nucleotides 2452–2534 from accession number M86379) (14). Prior to qPCR analysis, the reverse-transcription product from the non-treated sample was amplified to obtain cDNA for making a standard curve. The reaction was conducted as follows: 95°C for 20 s as a hold stage; 40 cycles at 95°C for 1 s and 60°C for 20 s as a PCR stage; and 95°C for 15 s, 60°C for 60 s, and 95°C for 15 s as a melt curve stage. All reactions were repeated in triplicate.

SDS-PAGE and mass spectrometer analysis Sodium dodecyl sulfate-polyacrylamide gel electrophoresis (SDS-PAGE) was carried out for UV₂₅₅- and UV₂₈₁-radiated FCVs. After subjecting samples to 20 mJ/cm² of UV-C radiation using each LED, 30 μ L of FCV was collected and incubated with 20 μ L of sample buffer (0.15 M Tris-HCl, 3% SDS, 30% glycerol, and 0.5% bromophenol blue) and a protein standard marker at 99°C for 5 min. The denatured virus solution was loaded on a 10% gel and electrophoresed with a solution containing 0.3% Tris, 0.1% SDS, and 1.44% glycine. After electrophoresis, the gel was stained by Coomassie brilliant blue, and the band intensity was measured with a gel imager. The band derived from the capsid protein (62 kDa) was excised and subjected to tryptic in-gel digestion. More specifically, the gel fractions were destained and dehydrated using 50% acetonitrile and 25 mM ammonium bicarbonate until the gel fractions were decolorized and were then dried using a centrifugal concentrator VC-15SP (TAITEC, Tokyo, Japan). Trypsin (10 ng/ μ L) in 50 mM ammonium bicarbonate was subsequently added and diffused into the gel fractions incubated on ice for over 30 min. The samples were digested overnight at 37°C. The peptides were first extracted from the polyacrylamide gel using 50 μ L of extraction liquid (50% acetonitrile and 5% trifluoroacetic acid) and then extracted again with 25 μ L of the same extraction liquid. The resultant extracts were completely evaporated and suspended in 20 μ L of extraction liquid for mass spectrometric analysis.

Each trypsin-digested peptide solution was analyzed by mass spectrometer (MS) using a direct nanoflow liquid chromatography (LC) system (DiNa; KYA Technologies, Tokyo, Japan) and an electrospray ionization (ESI) quadrupole time-of-flight MS (TripleTOF5600 system; AB Sciex). The peptide samples were prepared as indicated above and were introduced into a C18 reverse-phase chromatograph (C18 trap column: 1-mm long and 0.5-mm id; C18 separation column: 50-mm long and 0.1-mm id). The C18 column was washed with solvent A (2% acetonitrile and 0.1% v/v formic acid), and separation was conducted by application of a concentration gradient of 0–45% solvent B (80% acetonitrile and 0.1% v/v formic acid) for 30 min, followed by a linear gradient of 100% solvent B for 5 min at a flow rate of 300 nL/min. The eluted peptides were introduced online into a mass spectrometer by ESI with a 2.3 kV spray voltage. Positive ion intensities were recorded in TOF MS scan between

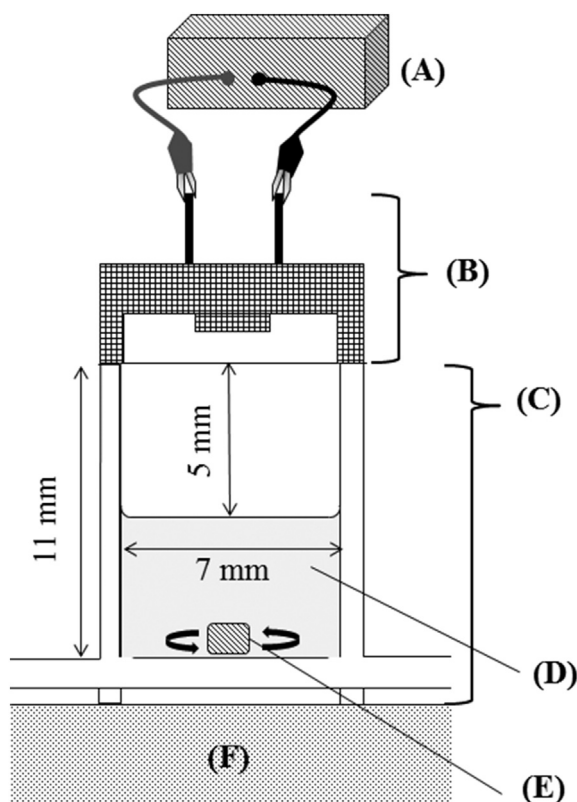


FIG. 1. Schematic view of the UV-C-LED radiation system. (A) Power supply for applying electric current; (B) UV-C-LED was operated at 255, 261, 277, or 281 nm; (C) well; (D) 180 μ L of FCV suspension; (E) micro-stirrer bar; (F) magnetic stirrer.

TABLE 1. Conditions for UV-C radiation using LEDs driving at 20 mA.

LED	Average irradiance rate (mW/cm ²)	Radiation time (s)	Fluence (mJ/cm ²)
UV ₂₅₅ -LED	0.235–0.259	~170	~40
UV ₂₆₁ -LED	0.168–0.180	~238	~40
UV ₂₇₇ -LED	0.629–0.696	~62	~40
UV ₂₈₁ -LED	0.704–0.759	~57	~40

Download English Version:

<https://daneshyari.com/en/article/6489717>

Download Persian Version:

<https://daneshyari.com/article/6489717>

[Daneshyari.com](https://daneshyari.com)